JOURNAL OF MAGNETIC RESONANCE **124,** 147–153 (1997)
ARTICLE NO. MN961022

Multidimensional Solid-State Nuclear Magnetic Resonance for Correlating Anisotropic Interactions under Magic-Angle Spinning Conditions

TOSHIMICHI FUJIWARA, TAIJI SHIMOMURA, AND HIDEO AKUTSU

Department of Bioengineering, Faculty of Engineering, Yokohama National University, 156 Tokiwadai, Hodogaya-ku, Yokohama 240, Japan

Received July 24, 1996; revised October 1, 1996

Multidimensional NMR spectroscopy has been developed for correlating anisotropic interactions of different spins in solids rotating at the magic angle. Anisotropic interactions, such as heteronuclear dipolar couplings and chemical-shift anisotropies, are recovered in the evolution periods by newly designed RF pulse sequences. Calculated spectra for this correlation experiment depended on the mutual orientation of tensorial interactions. Thus, this method can provide structural information, e.g., dihedral angles, for spin pairs distinguished by isotropic chemical shift. Experimental and numerically simulated results are presented for L-alanine fully labeled with ^{13}C nuclei. © 1997 Academic Press

INTRODUCTION

Two-dimensional correlation NMR spectra between anisotropic interactions in powdered solids contain information on relative orientations of tensorial interactions, e.g., the direction of a CH vector in the principal-axis system for a shielding tensor of the carbon (*1, 2*). Mutual orientations of such anisotropic interactions for different spins are relevant to three-dimensional structures of molecules. Two-dimensional correlation for different spins has been employed to evaluate relative directions of chemical bonds and functional groups in crystals and polymers (*3–8*). If such an orientation for carbons connected by a covalent bond is determined, information on the dihedral angle can be obtained (*9*). However, those 2D correlation experiments for different spins have been made under static or slow sample-spinning conditions, which entails low spectral resolution. This is a drawback for the analysis of molecules isotope-labeled at a number of sites.

We have shown that the spectral resolution for organic solids fully labeled with ^{13}C and ^{15}N can be improved by using another isotropic-shift axis in 2D experiments (*10*). In this work, we have added an isotropic-shift evolution period to a 2D experiment for correlating anisotropic interactions. This improvement in resolution extends the applicability of these correlation experiments to more complex molecules, for which signal overlap makes the measurement of the 2D correlation spectra for anisotropic interactions difficult.

The multidimensional experiment which includes isotropic-shift evolutions for resolving signals requires the evolution periods, each of which is dominated by a single type of anisotropic interaction under MAS (magic-angle spinning) conditions. In this study, we have developed RF multipulses for recovering chemical-shift anisotropy and CH dipolar interaction under MAS. These pulse sequences were applied to uniformly ^{13}C-labeled L-alanine. Experimental results for the correlation experiments with the multipulses are compared with numerical calculations to analyze the dependence on a dihedral angle.

THEORY AND RESULTS

Recovery of Chemical-Shift Anisotropy under MAS Conditions

The constant-time evolution period for ^{13}C shielding anisotropy under MAS includes only three π pulses as shown in Fig. 1a. Similar pulse sequences have been used to enhance and manipulate spinning sidebands due to shielding anisotropy (*11, 12*). Heteronuclear dipolar interactions are decoupled by an RF field for ^{1}H. Homonuclear dipolar couplings for ^{13}C are averaged by MAS during the constant-time period independently of t_1 (*13*), if the effects combined with chemical shifts are disregarded. The time-dependent shielding Hamiltonian $H_C(t)$ for a spin under a MAS condition is expressed by (*14*)

$$H_C(t) = [A + \sum_{m=1}^{2} \{C_{Cm}\cos(m\omega_R t) + S_{Cm}\sin(m\omega_R t)\}]S_z. \quad [1]$$

Here A is the isotropic shift, C_{Cm} and S_{Cm} depend on the molecular orientation relative to the static fields, S_z is the z component of the ^{13}C spin operator, and $\omega_R = 2\pi/\tau_R$. Coherent averaging of $H_C(t)$ in the toggling frame driven by RF pulses (*15*) gives the propagator for this period, $\exp(i\pi S_x)\exp(-iL_C)$ and

1090-7807/97 $25.00

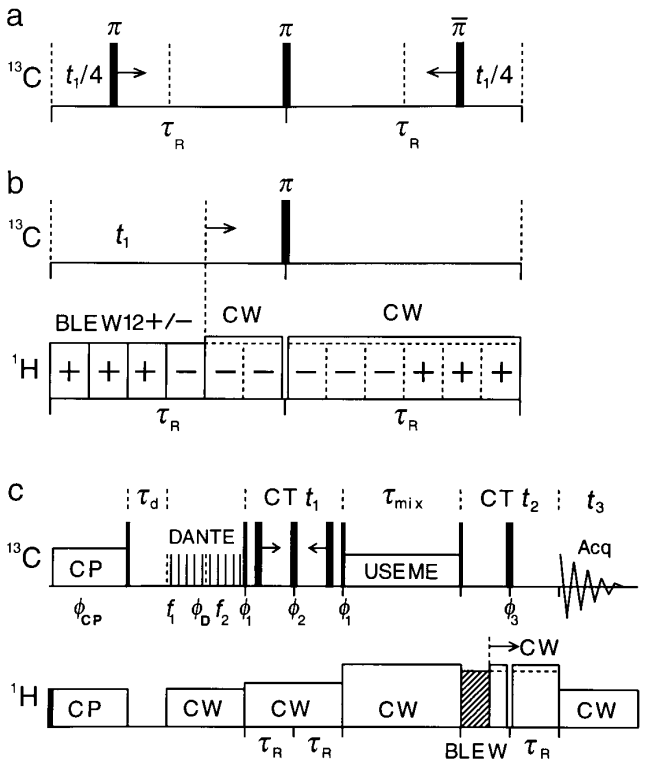

FIG. 1. (a) Constant-time evolution period for ^{13}C chemical-shift anisotropies under MAS conditions. The π pulses are separated by a sample-rotation period τ_R at $t_1 = 0$. The bar on the π pulse denotes a 180° phase shift. (b) Constant-time evolution period for CH dipolar couplings under MAS conditions. The pulse width of a BLEW12 sequence is $\tau_R/6$. The phases for $\pi/2$ pulses in BLEW12+ are $xy\bar{y}yxy\bar{y}\bar{x}y\bar{x}y$, and those in BLEW12− are $\bar{y}\bar{x}y\bar{x}\bar{x}y\bar{x}y\bar{y}yx\bar{y}$. (c) Pulse sequence for correlating anisotropic interactions under MAS. The initial z magnetization for ^{13}C is prepared by cross polarization (CP) and the following $\pi/2$ pulse is represented by a narrow dark pulse. Residual transverse magnetization dephases during the delay $\tau_D = 2$ ms. The DANTE $\pi/2$ pulses at C^α (f_1) and C^β (f_2) frequencies cancel the C^α and C^β magnetizations with their phase cycling. The t_1 and t_2 periods are the same as in (a) and (b), respectively. The RF phases are $\phi_{CP} = 16x16\bar{x}$, $\phi_D = \bar{y}yyy\bar{y}$, $\phi_1 = yy\bar{y}\bar{y}$, $\phi_2 = 4\bar{x}4x$, $\phi_3 = 8\bar{x}8x$, and $\phi_{Acq} = 16x16\bar{x}$. Three π pulses in the t_1 period are cycled synchronously with ϕ_2. The other pulses have constant phases.

$$L_C(t_1) = \left\{ + \int_0^{t_1/4} - \int_{t_1/4}^{\tau_R} + \int_{\tau_R}^{2\tau_R - t_1/4} - \int_{2\tau_R - t_1/4}^{2\tau_R} \right\} H_C(t)dt$$
$$= \frac{\tau_R}{\pi} \left\{ 2S_{C1}\left(1 - \cos\frac{\omega_R t_1}{4}\right) + S_{C2}\left(1 - \cos\frac{\omega_R t_1}{2}\right) \right\} S_z. \quad [2]$$

The π pulses determine the signs before the integrals. The isotropic shift is canceled. Only the terms which oscillate as $\sin \omega_R t$ and $\sin 2\omega_R t$ are recovered. The interval between the beginning of this period and the first π pulse is defined as $t_1/4$, so that the anisotropy having the time dependence of $\sin \omega_R t$ over an interval of $2\tau_R$ is recovered at $t_1 = 2\tau_R$. An effective Hamiltonian for this period, $L_C(t_1)/t_1$, is time dependent. As the π pulses move in the directions indicated in Fig. 1a from $t_1 = 0$ to $2\ \tau_R$, the factor for the first term $[1 - \cos(\omega_R t_1/4)]$ increases monotonically.

When this pulse sequence is applied to uniformly ^{13}C-labeled alanine at a ^{13}C resonance frequency of 100 MHz, the t_1 dependence of the magnetization is dominated by the shielding anisotropy, not by the ^{13}C homonuclear dipolar interactions. This is verified by the experimental results shown in Fig. 2a. The carboxyl signal reached zero intensity at $t_1 = 150\ \mu s$, whereas the $^{13}C^\beta$ signal stayed almost constant under the dipolar coupling with $^{13}C^\alpha$. Although the ^{13}C homonuclear dipolar splitting of about 3.2 kHz for a spin pair connected with a covalent bond is comparable to the shielding anisotropy of $^{13}C^\alpha$, $|\sigma_{33} - \sigma_{11}| = 3.4$ kHz, the t_1 dependence of the $^{13}C^\alpha$ magnetization calculated without the carbon dipolar couplings is consistent with the experimental dependence (Fig. 2b). The agreement between the experimental and calculated t_1 dependence for the carboxyl carbon is also shown in Fig. 2b. A π pulse train synchronized with sample rotation is known to recover ^{13}C homonuclear dipolar interactions when the chemical-shift differences are comparable to a sample-spinning frequency (*16*), but such effect on the t_1 dependence was small under our experimental conditions. The ^{13}C dipolar interactions would influence the evolution, however, when those dipolar interactions are larger than the shielding anisotropies.

Recovery of Heteronuclear Dipolar Interaction under MAS Conditions

The constant-time evolution period for recovering CH dipolar couplings under MAS is given in Fig. 1b. Another

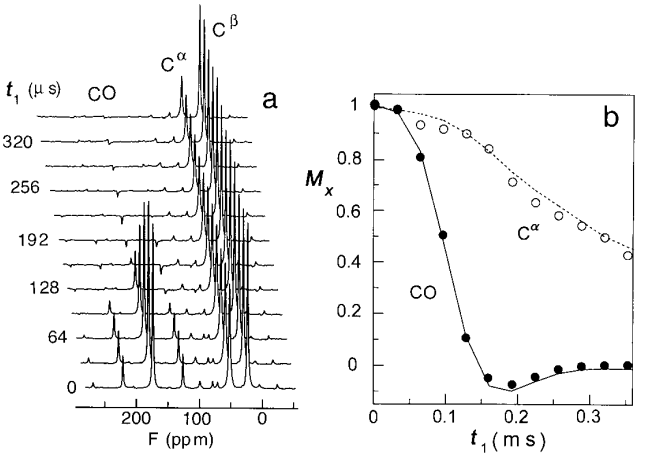

FIG. 2. (a) Experimental spectra of ^{13}C-labeled alanine, and (b) experimental and simulated signal intensities of the α and carboxyl carbons as a function of t_1 for the period shown in Fig. 1a. In (b), the experimental intensities of the α and carboxyl carbons are indicated by open and solid circles, respectively. The carboxyl signal intensities include the contribution of spinning sidebands. The dotted and solid lines connect the x components of the magnetization calculated for the $^{13}C^\alpha$ and ^{13}CO single-spin systems with $(\sigma_{11}, \sigma_{22}, \sigma_{33}) = (63, 72, 97)$ and $(-114, -55, 22)$ ppm (*22*), respectively.

constant-time evolution period without dipolar recoupling has been used to measure heteronuclear dipolar couplings from spinning sidebands (*17*). When $t_1 = 0$, a continuous wave field decouples CH dipolar couplings throughout the period. As t_1 increases, the CW decoupling is replaced with the homonuclear dipolar decoupling by BLEW12, during which the ^{13}C magnetization evolves under scaled CH dipolar interactions (*18*). To recover the CH dipolar couplings under MAS, the effective CH dipolar interaction is reversed synchronously with the sample rotation by BLEW12+ and −; the CH dipolar couplings during BLEW+ are different from those during BLEW− by a factor of −1. When the cycle time of BLEW is much shorter than τ_R, the time-dependent CH dipolar Hamiltonian under BLEW+/− can be expressed as

$$H_D(t) = \sum_{m=1}^{2} \{C_{Dm}\cos(m\omega_R t) + S_{Dm}\sin(m\omega_R t)\}[sk(t)\mathbf{n}\cdot\mathbf{I}]S_z. \quad [3]$$

Here s is the scaling factor for BLEW, $\mathbf{I}$ [$=(I_x, I_y, I_z)$] is the vectorial spin operator for ^1H, $\mathbf{n}$ is the unit vector specifying the direction of the spin operator resulting from the I_z operator averaged under BLEW, and $k(t) = 1$ and -1 are determined by BLEW+ and −, respectively.

An application of coherent-averaging theory to the period shown in Fig. 1b gives the propagator for a carbon spin $\exp(i\pi S_x)\exp(-iL_D)$, where

$$L_D(t_1) = \left\{ + \int_0^{\tau_R} - \int_{\tau_R}^{2\tau_R} \right\} H(t_1 - t)H_D(t)dt, \quad [4]$$

the Heaviside unit function $H(t_1 - t) = 1$ ($t < t_1$), $H(0) = \frac{1}{2}$, $H(t_1 - t) = 0$ ($t_1 < t$), and $k(t) = 1$ ($0 \leqslant t \leqslant \tau_R/2$, $3\tau_R/2 \leqslant t \leqslant 2\tau_R$), $k(t) = -1$ ($\tau_R/2 < t < 3\tau_R/2$) for $H_D(t)$. The effect of the heteronuclear dipolar interaction is cumulative even under MAS by this pulse sequence. When $t_1 = j\tau_R/2$ ($j = 0, 1, 2, 3, 4$), L_D is proportional to t_1 as $L_D(t_1) = 2t_1(S_{D1}/\pi)s\mathbf{n}\cdot\mathbf{I}S_z$. Only the dipolar term oscillating as $\sin \omega_R t$ is restored. The anisotropic shift is reduced to zero by MAS. The ^{13}C π pulse cancels the isotropic shift. The effects of the ^{13}C homonuclear dipolar interactions on the t_1 dependence of magnetization are much smaller than those of the $^{13}C^{\alpha}\,^1H^{\alpha}$ dipolar coupling as seen in the spectra of labeled alanine in Fig. 3a. The $^{13}C^{\alpha}$ transverse magnetization decayed much faster than the carboxyl magnetization that is under the influence of its large shielding anisotropy and ^{13}C homonuclear dipolar couplings. The transverse magnetization calculated for the $^{13}C^{\alpha}\,^1H^{\alpha}$ spin system without ^{13}C homonuclear couplings agrees with experimental signal intensity as shown in Fig. 3b.

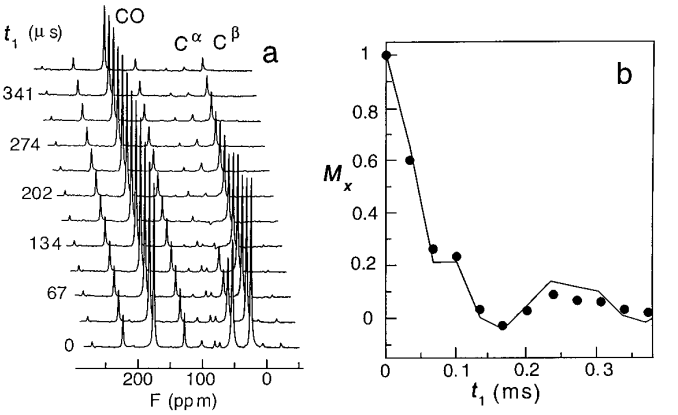

FIG. 3. Experimental spectra of ^{13}C-labeled alanine (a), and experimental and simulated signal intensities of $^{13}C^{\alpha}$ (b) as a function of t_1 for the period shown in Fig. 1b. The magnetization calculated is connected by solid lines.

Correlation of Anisotropic Interactions

Pulse sequences for the correlation experiments have two evolution periods for anisotropic interactions, which are connected by a mixing period. Specific spin pairs relevant to the correlation of the anisotropic interactions are selected by isotropic-shift evolutions. Figure 1c shows the pulse sequence used for the correlation between the carboxyl shielding anisotropy and the $C^{\alpha}H^{\alpha}$ dipolar interaction in ^{13}C-labeled alanine. The transverse carboxyl ^{13}C magnetization is selectively prepared with DANTE pulses (*19*) and precesses under the shielding anisotropy during the t_1 period. This magnetization is transferred to C^{α} by the ^{13}C homonuclear dipolar coupling with the mixing pulse USEME (*20*) during τ_{mix} in Fig. 1c. The C^{α} magnetization evolves under the $C^{\alpha}H^{\alpha}$ dipolar interaction during the t_2 period. Finally, the FIDs are acquired during the t_3 period for isotropic chemical shifts. The experimental spectrum obtained with this sequence is shown in Fig. 4a. The 2D cross section F_1/F_2 at the $^{13}C^{\alpha}$ resonance in F_3 is shown. The spectrum is symmetric with respect to the lines $F_1 = 0$ and $F_2 = 0$, because only real components were observed for the t_1 and t_2 dimensions and the imaginary parts having almost zero intensities were disregarded.

The spectra obtained with this correlation method are analyzed by numerical simulation. For static solids, time-independent eigenvalues of the Hamiltonian for evolution periods are correlated by the mixing of magnetization. In our experiment for rotating solids, sample spinning makes the spin Hamiltonian time dependent, so that the analysis of the 2D correlation spectra is not straightforward compared with that of the static spectra. However, the spectra for rotating solids are predictable through numerical calculation. The time dependence of magnetization during the evolution periods agreed with the numerical results as shown in Figs. 2

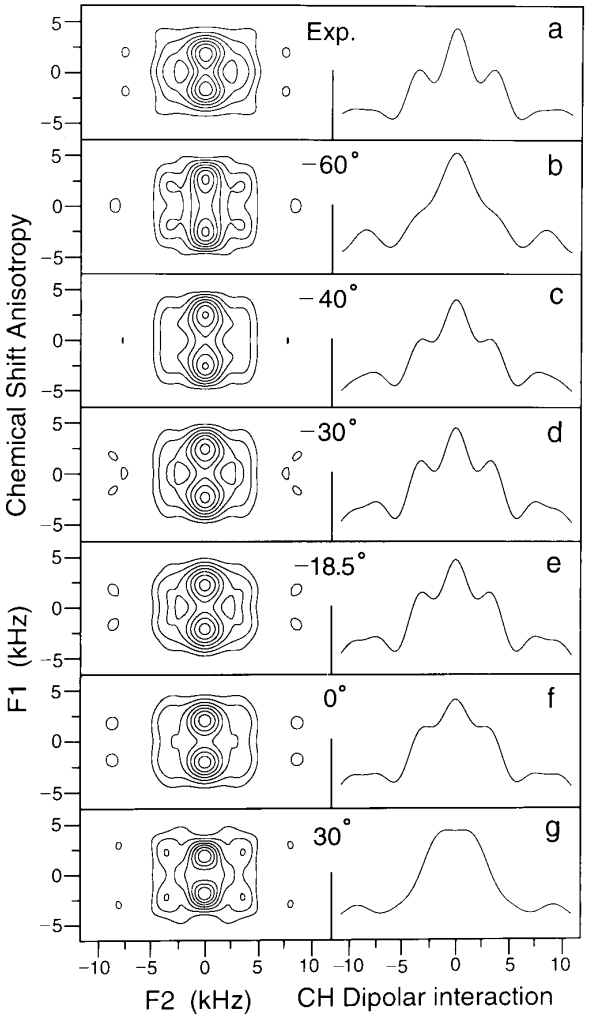

FIG. 4. Experimental (a) and simulated (b–g) 2D spectra for the correlation between the carboxyl ^{13}C shielding anisotropy (F_1) and the $^{13}C^{\alpha}{}^{1}H^{\alpha}$ dipolar coupling (F_2) for alanine. The cross sections were taken along the F_2 axis at $F_1 = 0$ kHz. The spectra (b–g) were calculated for the dihedral angles ψ described in the figures. The principal-axis system of the shielding anisotropy relative to the carboxyl local structure was assumed to be independent of ψ. The successive contour levels are different by a constant interval.

and 3. The mixing time of 1.2 ms for Fig. 4 is too short to reach a quasi-equilibrium state by the RF-driven spin diffusion (*6, 20*). This coherence of magnetization transfer was also taken into account by the numerical simulation. The simulated 2D spectra are shown in Figs. 4 and 6.

Figures 4b to 4g show the 2D spectra calculated for the dihedral angle ψ from −60° to 30°. Here, ψ is the rotation angle about the OC–C^{α} bond that is defined according to IUPAC conventions (*21*). The rotation by ψ changes the direction of the $C^{\alpha}H^{\alpha}$ vector relative to the σ_{22} and σ_{33} axes but not to the σ_{11} axis, because the σ_{11} axis is almost parallel to the OC–C^{α} bond (*22*) as shown in Fig. 5, where the orientations of the $C^{\alpha}H^{\alpha}$ vector are indicated. The experimental spectrum is similar to the spectra simulated for $\psi = -30°$ and −18.5° in that they have minima at about $(F_1, F_2) = (0, \pm 2.5)$ kHz as seen in the cross sections in Fig. 4. The other simulated spectra have no or very shallow minima. This leads to $-40° < \psi < 0°$ and denying $-60° < \psi < -40°$ and $0° < \psi < 30°$. The single-crystal analysis revealed that $\psi = -18.5°$ (*21*). Although we cannot determine the angle precisely, we can restrict the range of the dihedral angle.

The $C^{\alpha}H^{\alpha}$ vector relative to the σ_{11} axis is altered for Figs. 6a and 6b, the $C^{\alpha}H^{\alpha}$ vectors for which are shown in Fig. 5. The CH vector for A is tilted from the vector for $\psi = -18.5°$ to the σ_{11} axis by 17°. The vector for B is parallel to the C^{α}–CO bond. These simulated spectra in Figs. 4 and 6 indicate that the spectrum depends on the orientation of the $C^{\alpha}H^{\alpha}$ vector and is sensitive to the orientation with respect to the σ_{11} axis. Alternatively, if the molecular structure is known, information for the orientation of the principal axes of the shielding anisotropy with respect to the molecular structure can be obtained.

Fully labeled molecules can be analyzed with this method, because the 2D correlation spectra were insensitive to the presence of an additional ^{13}C–^{13}C dipolar coupling at a short mixing time. Figure 6c shows the spectrum simulated at $\psi = -18.5°$ for the four-spin system including the $^{13}C^{\beta}$ nucleus that covalently bonds to $^{13}C^{\alpha}$. This 2D spectrum is very similar to the spectrum for the three-spin system at $\psi = -18.5°$ (Fig. 4e). Since no cross peak for a spin pair separated by more than two covalent bonds was observed for a fully ^{13}C-labeled organic solid, adenosine, at a mixing time of 1.2 ms (*10*), ^{13}C–^{13}C spin interactions at longer distances have negligible effects at that mixing time. The evolution periods used are governed by the carboxyl shielding anisotropy and the $C^{\alpha}H^{\alpha}$ dipolar coupling as stated in the previous sections, so that the other ^{13}C spins in labeled molecules would not affect the evolutions.

DISCUSSION

The multidimensional correlation experiment proposed aims to improve spectral resolution and signal sensitivity by using isotropic-shift evolution under MAS. Under static conditions, it would not be easy to obtain the correlation between the carboxyl shielding anisotropy and the $C^{\alpha}H^{\alpha}$ dipolar coupling even from fully labeled alanine in powder, since its C^{α} and C^{β} signals overlap and the carboxyl signal is broadened by the shielding anisotropy (*22*) and carbon homonuclear dipolar couplings. As shown for alanine in this paper, as long as signals are resolved by MAS, multiply labeled molecules can be analyzed with this method. This is especially beneficial to biological samples, since the preparation of uniformly labeled molecules has been established (*10, 23*).

In the simulation, we have shown that, even if the number

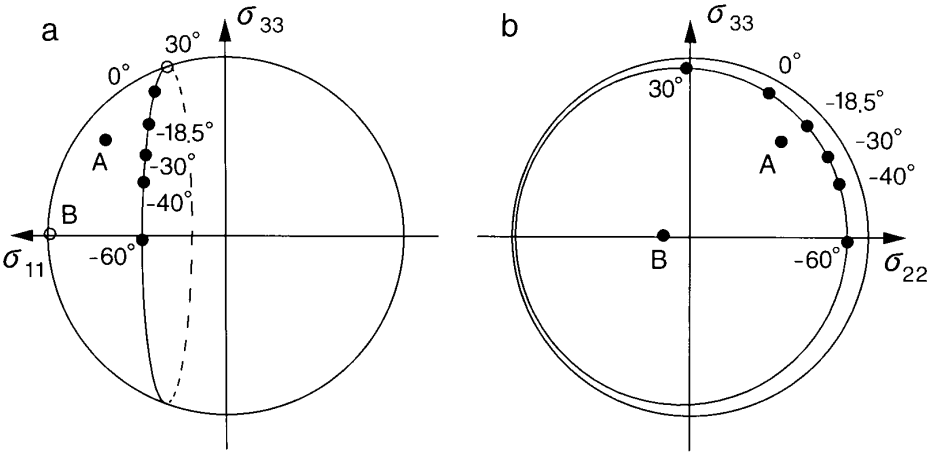

FIG. 5. Orientations of the $C^{\alpha}H^{\alpha}$ unit vectors relative to the principal axes of the carboxyl chemical-shift tensor for Figs. 4b to 4h and 6a to 6c. The points on the unit sphere indicate the vectors, and are projected onto the $\sigma_{11}\sigma_{33}$ and $\sigma_{22}\sigma_{33}$ planes in (a) and (b), respectively. The solid and open circles denote positive and negative values, respectively, for the coordinates perpendicular to the planes. The trajectory of the CH vector for the dihedral angle $-180° < \psi \leqslant 180°$ is represented by solid and dashed lines for positive and negative values. Dihedral angles for the points are shown on the figures. See the legend to Fig. 6 for points A and B.

of time points was 10 for each of the t_1 and t_2 dimensions, the spectra were sensitive to the relative orientation of anisotropic interactions. Such a small number of time points leads to a short experimental time, and is useful for improving the resolution by increasing the dimensionality of NMR. The selective pulses in the preparation period of the sequence (Fig. 1c) can be replaced with an isotropic-shift evolution period to obtain information for more spin pairs. Such a 4D experiment requires a longer experimental time for the isotropic-shift evolution, and limits the number of time points for the periods of the anisotropic interactions.

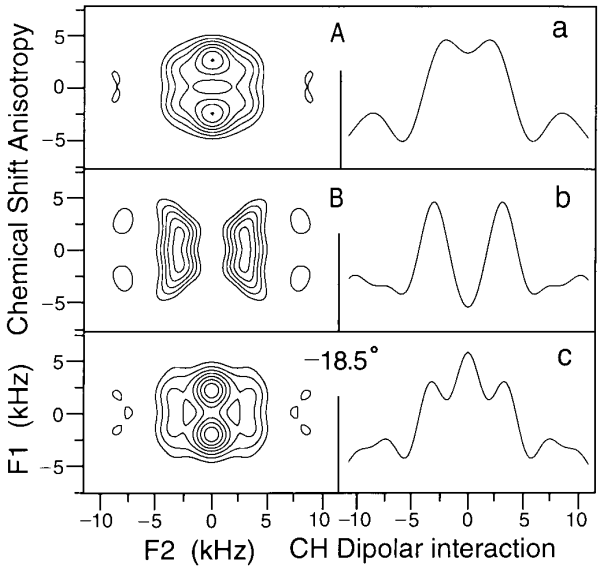

FIG. 6. Simulated 2D spectra for the correlation between the carboxyl ^{13}C shielding anisotropy and the $^{13}C^{\alpha}{}^{1}H^{\alpha}$ dipolar coupling. For (a) and (b), the relative orientations are indicated by points A and B in Fig. 5, respectively. Spectrum (c) was calculated at $\psi = -18.5°$ for the four-spin system.

Mechanical switching of the sample-spinning axis (*2, 24*) can be utilized to recover anisotropic interactions as well as RF pulses synchronized with sample spinning. We have, however, employed the method using the RF pulses, because such pulse experiments can be performed with a conventional MAS probe. Some pulse sequences for the evolution of anisotropic interactions have a dwell time of sample rotation period τ_R (*25, 26*). When these pulse sequences are applied to anisotropic interactions much larger than the sample-spinning frequency, the pulse sequences must also reduce the interactions to less than the spectral width that is equal to $1/\tau_R$. Such a reduction needs a longer evolution period which is generally vulnerable to other effects due to interactions such as ^{13}C homonuclear coupling and RF field inhomogeneity. Under our experimental conditions, the carboxyl shielding anisotropy and the CH dipolar interaction under the BLEW sequence are about 14 and 11 kHz, respectively, and are larger than the spinning frequency of 5 kHz. We have, therefore, used other types of evolution periods which have dwell times of less than τ_R and do not necessitate the reduction.

Several NMR phenomena under rotational resonance conditions have been shown to depend on dihedral angles as results of the correlation between two shielding anisotropies (*9, 27*). Multidimensional NMR allows us to make different correlations of anisotropic interactions (*1*) which are sensitive to the structural parameters. One example is a correlation experiment having two CH dipolar evolution periods shown in Fig. 1b. The principal axes of the dipolar interaction are specified by the direction of the CH bond, while those of the carboxyl shielding anisotropy are not completely deter-

mined by the directions of the $C^{\alpha}-CO$ and $C-O$ bonds and are slightly ambiguous owing to their dependence on hydrogen bonds and dihedral angles (*28*). This is an advantage of the CH−CH correlation over the correlation including the shielding anisotropy in obtaining dihedral angle information.

We have shown the applicability of this method to an amino acid, alanine, in this paper. This method can be used for obtaining the information of ψ also for peptides, since the relative orientations of the anisotropic interactions in peptides depend on ψ similarly to that in alanine (*22, 29*).

High-precision information on the dihedral angle ψ would be obtained from the correlation spectra having higher resolution in the frequency axes for the anisotropic interactions, although the measurement needs more experimental time to increase the number of time points for those dimensions. Additional correlation experiments can also be made to reduce the range of ψ. An experiment for correlating the $^{13}C^{\alpha}$ shielding anisotropy with the carbonyl ^{13}C anisotropy would also give information on ψ. Spectra for the correlation between carbonyl ^{13}C shielding anisotropies of the neighboring amino acid residues in peptides were recently shown to be sensitive to ψ (*8*).

In the structural determination of molecules by solution NMR, constraints on dihedral angles derived from three-bond J coupling constants complement internuclear distances estimated from NOE intensities (*23*). Similarly in solids, dihedral angle information obtained by the method presented in this paper will contribute to the determination together with internuclear distances measured for isotope-labeled molecules under MAS conditions (*30*).

EXPERIMENTAL

Experiments were performed on an Otsuka Electronics CMX 400 spectrometer with a probe for a 5 mm rotor at a static magnetic field of 9.4 T. Initial ^{13}C magnetization was prepared by cross polarization with a contact time of 1 ms. The ^{13}C π pulse widths were 5.0 μs. The MAS frequency was about 4950 Hz. The $\pi/2$ pulse width for the homonuclear decoupling pulse BLEW was 2.8 μs. Proton CW decoupling strength was 65 kHz during the observation and 95 kHz during the $^{13}C-^{13}C$ mixing period. The experimental time was about four hours for the 3D experiment (Fig. 1c). A data matrix $10(t_1) \times 10(t_2) \times 512(t_3)$ acquired was zero-filled to a $128 \times 128 \times 512$ matrix and Fourier transformed with MSI Felix950. The powdered sample consisted of fully ^{13}C-labeled L-alanine and natural-abundance L-alanine in the ratio 1:9. Crystals of the alanine were grown from a saturated aqueous solution.

The structural and NMR parameters for defining spin systems for calculations were determined according to Refs. (*21, 22*) for single-crystal alanine. The evolution of the spin systems was calculated by the numerical integration of a time-dependent Hamiltonian, including terms for isotropic and anisotropic chemical shifts, and dipolar and J interactions (*20, 31*). A time evolution period was divided into piecewise sections, and its Hamiltonian was assumed to be time independent during each section. The sections began at intervals of about 1.7 μs and also at every RF phase shift, and gate-on and -off timings. Thus, a propagator for a 2π sample rotation was expressed as a product of about 130 propagators. Finite RF amplitudes were used. In the simulation of 2D cross sections, the propagators from the $\pi/2$ pulse at the beginning of the t_1 period to the end of the t_2 period were calculated, and they transformed the initial state of the carboxyl longitudinal spin operator. The final density matrix was projected onto the $^{13}C^{\alpha}$ transverse spin operator to obtain the time-domain signal. A two-step phase cycle different only in $\phi_1 = (x, -x)$ in Fig. 1c was employed. The signals with $10(t_1) \times 10(t_2)$ points for about 1400 orientations were added with a constant weight factor to generate a powder pattern (*2*). Further increases in the numbers of the time sections and orientations have negligible effects. The three-spin system for simulating 2D cross sections consisted of carboxyl ^{13}C, $^{13}C^{\alpha}$, and $^{1}H^{\alpha}$, and the four-spin system included additional $^{13}C^{\beta}$. The computational time for a spectrum was about 5 hours for the three-spin system and 30 hours for the four-spin system with a SGI Indigo2 workstation having an R4400 processor. To reduce the computational time, parts of the propagators calculated for the initial t_1 and t_2 values were stored, and were reused to calculate the propagators for the other t_1 and t_2 values.

CONCLUSIONS

The constant-time evolution periods were designed for recovering ^{13}C shielding anisotropy and CH dipolar couplings under MAS conditions. The recovery was verified by the experiments. These evolution periods were used in the pulse sequence for the 3D correlation experiment.

The experimental spectrum of alanine for the correlation between the carboxyl shielding anisotropy and the $C^{\alpha}H^{\alpha}$ dipolar interaction qualitatively agreed with the spectra simulated for the dihedral angle ψ approximately equal to that of the single-crystal structure. We have shown that the multidimensional NMR experiment with rotation-synchronized multipulses can provide information on the mutual orientation of anisotropic interactions and the dihedral angle as long as signals are resolved by the isotropic shift under MAS conditions.

ACKNOWLEDGMENTS

This research was partially supported by Grants-in-Aid for Specially Promoted Research (05101004, H.A.), Scientific Research of Priority Area and Large-Scale Research Project under the New Program System from the Ministry of Education, and by a grant from Kanagawa Academy of Science and Technology.

REFERENCES

1. M. Linder, H. Höhener, and R. R. Ernst, *J. Chem. Phys.* **73,** 4959 (1980).
2. T. Nakai, J. Ashida, and T. Terao, *J. Chem. Phys.* **88,** 6049 (1988).
3. D. P. Weliky, G. Dabbagh, and R. Tycko, *J. Magn. Reson. A* **104,** 10 (1993).
4. G. Dabbagh, D. P. Weliky, and R. Tycko, *Macromolecules* **27,** 6183 (1994).
5. P. Robyr, B. H. Meier, P. Fisher, and R. R. Ernst, *J. Am. Chem. Soc.* **116,** 5315 (1994).
6. P. Robyr, M. Tomaselli, J. Straka, C. Grob-Pisano, U. W. Suter, B. H. Meier, and R. R. Ernst, *Mol. Phys.* **84,** 995 (1995).
7. K. Schmidt-Rohr, *J. Am. Chem. Soc.* **118,** 7601 (1996).
8. D. P. Weliky and R. Tycko, *J. Am. Chem. Soc.* **118,** 8487 (1996).
9. Y. Tomita, E. J. O'Connor, and A. McDermott, *J. Am. Chem. Soc.* **116,** 8766 (1994).
10. T. Fujiwara, K. Sugase, M. Kainosho, A. Ono, A. (M.) Ono, and H. Akutsu, *J. Am. Chem. Soc.* **117,** 11351 (1995).
11. T. Gullion, *J. Magn. Reson.* **85,** 614 (1989).
12. O. N. Antzutkin, S. C. Shekar, and M. H. Levitt, *J. Magn. Reson. A* **115,** 7 (1995).
13. A. Bax and R. Freeman, *J. Magn. Reson.* **44,** 542 (1981).
14. M. M. Mariq and J. S. Waugh, *J. Chem. Phys.* **70,** 3300 (1979).
15. J. S. Waugh, *J. Magn. Reson.* **50,** 30 (1982).
16. D. K. Sodickson, M. H. Levitt, S. Vega, and R. G. Griffin, *J. Chem. Phys.* **98,** 6742 (1993).
17. J. E. Roberts, G. S. Harbison, M. G. Munowitz, J. Herzfeld, and R. G. Griffin, *J. Am. Chem. Soc.* **109,** 4163 (1987).
18. D. P. Burum, M. Linder, and R. R. Ernst, *J. Magn. Reson.* **44,** 173 (1981).
19. G. A. Morris and R. Freeman, *J. Magn. Reson.* **29,** 433 (1978).
20. T. Fujiwara, A. Ramamoorthy, K. Nagayama, K. Hioka, and T. Fujito, *Chem. Phys. Lett.* **212,** 81 (1993).
21. M. S. Lehmann, T. F. Koetzle, and W. C. Hamilton, *J. Am. Chem. Soc.* **94,** 2657 (1972).
22. A. Naito, S. Ganapathy, K. Akasaka, and C. A. McDowell, *J. Chem. Phys.* **74,** 3190 (1981).
23. G. M. Clore and A. M. Gronenborn, *in* ''Methods in Enzymology'' (T. L. James and N. J. Oppenheimer, Eds.), Vol. 237, p. 349, Academic Press, San Diego, 1994.
24. M. Tomaselli, B. H. Meier, M. Baldus, J. Eisenegger, and R. R. Ernst, *Chem. Phys. Lett.* **225,** 131 (1994).
25. Y. Yarim-Agaev, P. N. Tutunjian, and J. S. Waugh, *J. Magn. Reson.* **47,** 51 (1982).
26. R. Tycko, G. Dabbagh, and P. A. Mirau, *J. Magn. Reson.* **85,** 265 (1989).
27. T. Nakai and C. A. McDowell, *J. Magn. Reson. A* **112,** 199 (1995).
28. N. Asakawa, S. Kuroki, H. Kurosu, I. Ando, A. Shoji, and T. Ozaki, *J. Am. Chem. Soc.* **114,** 3261 (1992).
29. M. D. Lumsden, R. E. Wasylishen, K. Eichele, M. Schindler, G. H. Penner, W. P. Power, and R. D. Curtis, *J. Am. Chem. Soc.* **116,** 1403 (1994).
30. A. E. Bennett, R. G. Griffin, and S. Vega, *NMR Basic Principles Progress* **33,** 1 (1994).
31. A. Ramamoorthy, T. Fujiwara, and K. Nagayama, *J. Magn. Reson. A* **104,** 366 (1993).